Indian Journal of Chemistry
Vol. 61, March 2022, pp. 254-262

Syntheses, spectral characterization and antidiabetic activities of oxidovanadium(V) complexes with bi-and tridentate ligands

Neetu Patel, A K Patel, A K Prajapati* & R N Jadeja*

Department of Chemistry, Faculty of Science, The Maharaja Sayajirao University of Baroda, Vadodara 390 002, India

*E-mail: rjadeja-chem@msubaroda.ac.in

Received 30 September 2021; revised and accepted 10 February 2022

Four new oxidovanadium(V) complexes [VO(L^1)(Mol)] (**1**), [VO(L^2)(Mol)] (**2**), [VO(L^3)(Mol)] (**3**) and [VO(L^4)(Mol)] (**4**) (where L^1-L^4 = aroylhydrazones and Mol = maltol) have been synthesized with different ligands. The complexes have been characterized using microanalysis, spectral fab mass, UV-visible, electrochemical (cyclic voltammetry and differential pulse voltammetry), density functional theory calculations have been performed to predict the optimized geometry, global reactivity parameters and electron density. In these complexes, the d-d absorption band is not observed as being d^0 vanadium centres in these complexes. The electrochemical behaviour of these complexes are explored by cyclic voltammetry and differential pulse voltammetry (DPV). All complexes exhibit one electron transfer i.e., reduction of vanadium(V) to vanadium(IV). These complexes are screened for *in vitro* α-glucosidase and α-amylase inhibition study. Complex **3** has an interesting insulin-like activity.

Keywords: Oxidovanadium(V) complexes, Aroylhydrazone ligand, Density functional Theory, Antidiabetic activity

Vanadium distributes widely in nature and manifests several biological effects[1,2]. A number of vanadium compounds have diverse pharmacological and physiological effects like antidiabetic, anti-inflammatory, antiviral and anti-bacterial effects[2-4]. Vanadium compounds are suitable candidates in search of novel orally active chemotherapeutics as an alternative for the existing hypoglycaemic medicines[3,4]. The ethyl maltol vanadium complex has enrolled the phase II clinical trials. Additionally, studies on this complex as an antidiabetic agent were abandoned owing to renal problems, however, it is recently studied as a therapeutic for the prevention, stoppage reparation of secondary tissue injuries. Picolinato vanadium complexes were also found to have strong antidiabetic features. A number of picolinato scaffold have been synthesized viz., 5-methepiconate, 6-ethylpiconate, halopiconates, 3-hydroxy piconates etc. which coordinate with vanadium and exhibit insulin mimetic properties.

Hydrazone Schiff bases have attracted significant attention owing to their diverse applications such as in liquid crystal[5,6], organic dyes[7], catalysts[8] and as intermediate for many bioactive molecules[9]. These organic compounds have been reported to bear many biological activities like anticancer[10], antibacterial[11], antituberculosis[13], anticonvulsant[14], antioxidant[15] and diuretic properties[16]. In addition, hydrazone Schiff base containing maltol complexes are used in a number of enzymatic biochemical reactions and also exhibited a range of bioactivities and applications[5,6]. The above facts have advised the synthesis of new vanadium complexes with high bioavailability and low toxicity.

Herein, we report four vanadium complexes synthesized from ONO hydrazone Schiff base as pro-ligand and maltol as co-ligand viz., [VO(L^1)(Mol)] (**1**), [VO(L^2)(Mol)] (**2**), [VO(L^3)(Mol)] (**3**) and [VO(L^4)(Mol)] (**4**) (where L^1-L^4 = aroylhydrazones ligands and Mol = maltol). These complexes were characterized using microanalysis and several spectral physico-chemical techniques. Computational density functional theory has been used to establish the stable geometrical form of used ligand and its complexes. Quantum computational density functional theory (DFT) has also yielded significant electronic structural parameters. The insulin mimetic activity *in vitro* has also been investigated.

Experimental Details

Materials and physical measurements

$VOSO_4.5H_2O$ (Across Organics), 2,2'-bis (pyridylmethyl)amine (Aldrich), 1,10-phenanthroline (S.D. Fine), 2,2-bipyridyl (CDH), Maltol (Sigma

Aldrich), Ethyl Maltol (Sigma Aldrich), and DMSO (S.D. Fine) were reagent grade and used as purchased from commercial sources without any further purification. The electronic absorption spectra (300–900 nm) were recorded with a Shimadzu UV-visible recording spectrophotometer UV-1601 in DMSO solution. Infrared (IR) spectra were recorded on a Perkin Elmer Fourier transform IR (FTIR) spectrum RX 1 Spectrometer as KBr pellets. Elemental analyses of C, H and N were determined using a Perkin Elmer series-II 2400 elemental analyzer. Electrochemical data were collected using a BAS-100 Epsilon Electrochemical Analyzer on compounds **1-4** in the DMSO solution using Ag/AgCl as a reference electrode and glassy carbon as a working electrode. Tetrabutylammonium perchlorate (TBAP) was used as a supporting electrolyte. ESI-mass spectra were recorded on Waters Q-ToF micro mass. Molar conductivities of the freshly prepared 1.0×10^{-3} M DMSO solutions were measured on a Systronics Conductivity 308 TDS meter.

Synthesis

Synthesis of [VO(L^1)(Mol)] 1

To a MeOH solution (20 mL) of (5-nitrosalicylaldehyde (0.167 g, 1.00 mmol) and benzhydrazide (0.136 g, 1.00 mmol) for **1**), (5-bromosalicylaldehyde (0.167 g, 1.00 mmol), and 3-hydroxylbenzohydrazide (0.152 g, 1.00 mmol) for **2**), (5-chlorosalicylaldehyde (0.156 g, 1.00 mmol) and 3-hydroxylbenzohydrazide (0.152 g, 1.00 mmol) for **3**) and (5-chlorosalicylaldehyde (0.156 g, 1.00 mmol) and 3-hydroxylbenzohydrazide (0.152 g, 1.00 mmol) for **4**) was added and the resulting solution was heated to reflux for 1 h at 75 °C. The reaction mixture was cooled at room temperature. To this solution, maltol (0.126 g, 1.00 mmol) and $VOSO_4$ (0.163 g, 1.00 mmol) dissolved in MeOH were added. The reaction mixture was further stirred for 3 h to give a brown solution and allowed to evaporate slowly in the air. After one weak, dark brown product separated, this was filtered and dried in a calcium chloride desiccator.

Yield: 72 %. Anal. Calc. for $C_{20}H_{14}N_3O_8V$ (M = 475.02 g mol^{-1}): C, 50.54; H, 2.97; N, 8.84 %. Found: C, 50.57; H, 2.99; N, 8.82 %. FTIR (KBr, cm^{-1}): ν(C=O) 1632 vs, ν(C=N) 1604 vs, ν(V=O) 952 vs, ν(V-O) 432 m, ν(V-N) 417 cm^{-1}. ESI Mass (m/z) = 475.73.

Synthesis of [VO(L^2)(Mol)] 2

Yield: 75 %. Anal. Calc. for $C_{20}H_{14}BrN_2O_7V$ (M = 525.18 g mol^{-1}): C, 45.74; H, 2.69; N, 5.33 %. Found: C, 45.76; H, 2.65; N, 5.36. %. FTIR (KBr, cm^{-1}): ν(C=O) 1621 vs, ν(C=N) 1596 vs, ν(V=O) 975 vs, ν(V-O) 484 m, ν(V-N) 445 cm^{-1}. ESI Mass (m/z) = 524.85.

Synthesis of [VO(L^3)(Mol)] 3

Yield: 78 %. Anal. Calc. For $C_{20}H_{14}ClN_2O_7V$ (M = 480.73 g mol^{-1}): C, 49.97; H, 2.94; N, 5.83 %. Found: C, 49.99; H, 2.96; N, 5.81 %. FTIR (KBr, cm^{-1}): ν(C=O) 1632, ν(C=N) 1606 vs, ν(V=O) 972 vs, ν(V-O) 459 m, ν(V-N) 409 cm^{-1}. ESI Mass (m/z) = 481.97.

Synthesis of [VO(L^4)(Mol)] 4

Yield: 76 %. Anal. Calc. for $C_{18}H_{18}ClN_2O_6V$ (M = 444.74 g mol^{-1}): C, 48.61; H, 4.08; N, 6.30 %. Found: C, 48.64; H, 4.10; N, 6.33 %. FTIR (KBr, cm^{-1}): ν(C=O) 1633 vs, ν(C=N) 1605 vs, ν(V=O) 973 vs, ν(V-O) 444 m, ν(V-N) 410 cm^{-1}. ESI Mass (m/z) = 446.94.

Antidiabetic activity

α-Glucosidase inhibition activity

The α-glucosidase inhibitory activity assay was performed as described previously[17]. In brief, rat-intestinal acetone powder was dissolved in 100 mL of saline water and sonicated properly at 4 °C. After sonication, the suspension was centrifuged (3,000 rpm, 4 °C, 30 min) and the resulting supernatant was used for the assay. A reaction mixture containing 50 µL of phosphate buffer (50 mM; pH 6.8), 50 µL of rat α-glucosidase and 50 µL sample of varying concentrations (100-800 µg/ mL) was pre-incubated for 5 min at 37 °C, and then 50 µL of 3 mM pNPG was added to the mixture as a substrate. After incubation at 37 °C for 30 min, enzymatic activity was quantified by measuring the absorbance at 405 nm in a microtiter plate reader (Bio-TEK, USA). Acarbose was used as a reference and experiments were carried out in triplicate. The inhibition percentage (%) was calculated as follows:

$$\% \text{ inhibition} = \frac{[A_C - A_S]}{A_C} \times 100$$

where A_C is the absorbance of the control and A_S is the absorbance of the tested sample. The concentration of inhibitor required to inhibit fifty percent of enzyme activity under the mentioned assay conditions is defined as the IC_{50} value.

α-Amylase inhibition activity

Pancreatic α-amylase assay was adopted from Apostolidis *et al*.[18]. 50 µL of different dilutions of test compounds and 50 µL of 0.02 M sodium phosphate

buffer (pH 6.9 with 0.006 M sodium chloride) containing α-amylase solution (0.5 mg/ mL) were incubated at 25 °C for 10 min. After pre-incubation, 50 µL of 1% starch solution in 0.02 M sodium phosphate buffer (pH 6.9 with 0.006 M sodium chloride) was added to each tube. The reaction was incubated at 25 °C for 10 min. The reaction was stopped with 100 µL of DNS colour reagent. The microplate was incubated (85-90 °C) for 10 min to develop colour and left to cool at room temperature. The reaction mixture was diluted with 105 µL of distilled water. Enzymatic activity was quantified by measuring the absorbance at 540 nm in a microtiter plate reader (Bio-TEK, USA). Acarbose was used as standard and experiments were done in triplicates. Acarbose was used as a reference.

Results and Discussion

Synthesis and spectroscopic properties

The oxidovanadium(V) complexes **1-4** [VO(L^{1-4})(Mol)] (L^{1-4} are four tridentate ligands and maltol). The tridentate L^{1-4} aroyl hydrazones ligands have not been pre isolated (L^1 = (E)-N'-(2-hydroxy-5-nitrobenzylidene)benzohydrazide, L^2 = (E)-N'- (5-bromo-2 hydroxybenzylidene)-3-hydroxybenzohydrazide, L^3 = (E)-N'-(5-chloro-2-hydroxybenzylidene)-3-hydroxy-benzohydrazideand L^4 =(E)-N'-(5-chloro-2-hydroxy-benzylidene) pivalohydrazide). *In situ* syntheses of aroyl hydrazones are shown in Scheme 1. The complexes have been isolated in good yield from a single step reaction of salicylaldehyde, hydrazides, $VOSO_4$ and maltol in a mixture of solvents using air as an oxidizing agent. The automatic oxidation is due to lowering of the reduction potential at the vanadium centre owing to OO^- ion coordination. The five negative charges appear from the phenolate oxygen O1(-1), the enolate oxygen O2 (-1), the oxo oxygen O3(-2) of tridentate hydrazone and oxygen O4(-1) of maltol. The synthetic routes of complexes are shown in Scheme 1. These complexes were characterized by elemental analysis, FTIR, UV-visible, CV and DPV. All the complexes are air-stable. The complexes are insoluble in water, hexane, benzene, and petroleum ether but soluble in DMSO, DMF, and acetonitrile. Molar conductivity (Λ_m/s) of value for complexes **1-4** are non-electrolytic in nature having a value in the range of 27.52-38.50 Ω^{-1} cm^2 mol^{-1}[119].

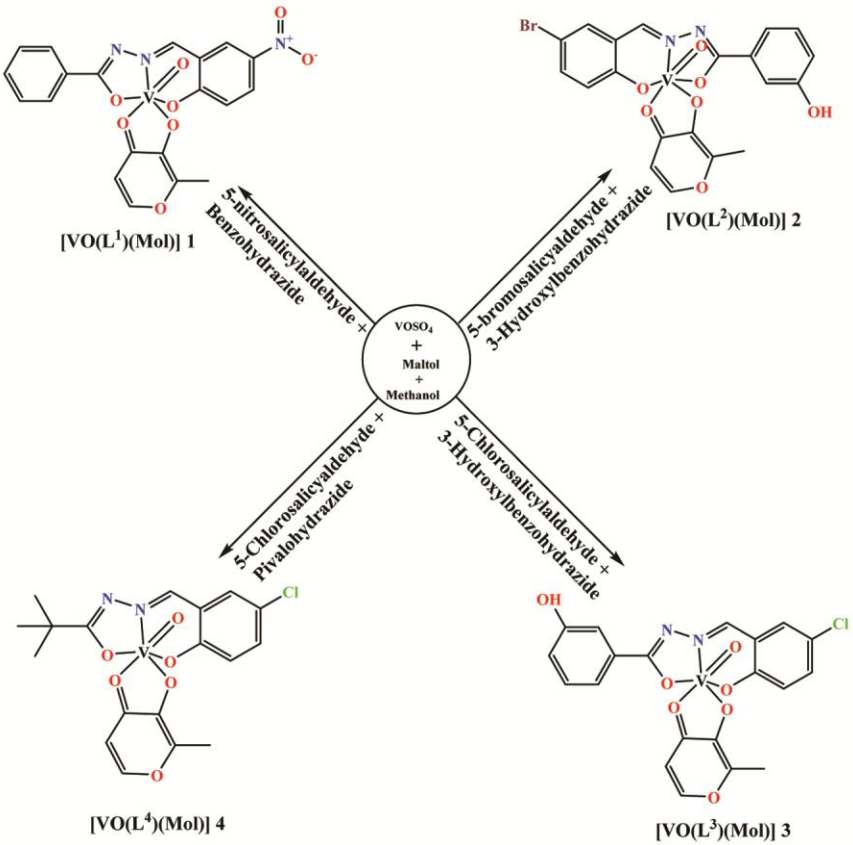

Scheme 1 — Synthetic route of complexes **1-4**

FTIR spectral study

In the FTIR spectra of complexes (**1-4**) the free aroyl hydrazone ligands exhibit bands in the spectral regions 3020-3185 cm^{-1} due to N-H stretching vibrations, respectively[20]. The FTIR data of complexes are given in Table 1. These absorption bands are absent in the present complexes, indicating the conversion of carbonyl moiety to an enolic moiety and resulting replacement of the phenolic moiety to enolic hydrogens[21]. A new band is present at the 1289-1303 cm^{-1} region in the complexes assigned to the ν(C-O) (enolato) stretching mode[22]. The absorption bands in the 1596-1606 cm^{-1} range, indicate the coordination of azomethine nitrogen to the vanadium. Moreover, the band in the regions 432-484, and 410-417 cm^{-1} can be attributed to the stretching modes of the vanadium to ligand bonds, ν(V-O) and ν(V-N), respectively. Besides, the complexes show a strong band in the 952-975 cm^{-1} range owing to the complexes due to the terminal V=O stretching, reveals a hexacoordinated sphere around the vanadium center[23]. The FTIR spectra of complexes **1-4** are shown in Fig. S1, Supplementary Data.

ESI mass analysis

As single crystals of complexes, **1-4** could not obtained so an ESI mass of complexes were done to confirm the molecular weight of complexes. Positive mode ESI-mass of complexes were done. The ESI mass of complexes is almost similar to the calculated mass of the complexes. The mass of complexes was obtained in $[M + 1]^+$ and $[M + 2]^+$ mode. The mass spectra of complexes are given in Fig. S2, Supplementary Data.

Electronic spectral study

UV-visible spectra of all complexes were recorded in DMSO solution (1.0×10^{-3} M). The UV-visible spectra of all complexes have similar spectral features. In the electronic spectra of complexes **1-4,** the bands in the range 312-326 nm are due to the intra ligand absorption of the azomethine group[24]. In all complexes, an intense absorption band at 401-409 nm is assigned to the phenolic $N_{(p)}/O_{(p)} \rightarrow V_{(dx)}$ ligand to metal charge transfer (LMCT) band[25]. The LMCT bands arise from the p-orbital lone pair of nitrogen/oxygen donor atoms of Schiff base to an empty d-orbital on the vanadium(V) centre[26]. Oxidovanadium(V) complexes exhibit bands at 312 nm (11236 $dm^3\ mol^{-1}\ cm^{-1}$), 409 nm (1244 $dm^3\ mol^{-1}\ cm^{-1}$) for **1**, 329 nm (11396 $dm^3\ mol^{-1}\ cm^{-1}$), 413 nm (2784 $dm^3\ mol^{-1}\ cm^{-1}$) for **2**, 325 nm (6871 $dm^3\ mol^{-1}\ cm^{-1}$), 410 nm (1748 $dm^3\ mol^{-1}\ cm^{-1}$) for **3** and 326 nm (6242 $dm^3\ mol^{-1}\ cm^{-1}$), 401 nm (3665 $dm^3\ mol^{-1}\ cm^{-1}$) for **4**, respectively. The d-d absorption bands were not observed in all complexes being d^0 vanadium systems as shown in Fig. 1.

Electrochemical studies of complexes

The electrochemical properties of complexes **1-4** were also studied at room temperature by cyclic voltammetry (CV) and differential pulse voltammetry (DPV) in DMSO containing 0.1 M tetrabutyl-ammonium perchlorate (TBAP) as a supporting electrolyte. The reduction potential data are summarized in Table 2. The cathodic peak potentials are found at -(0.6271-0.7085 V) as shown in Fig. 2.

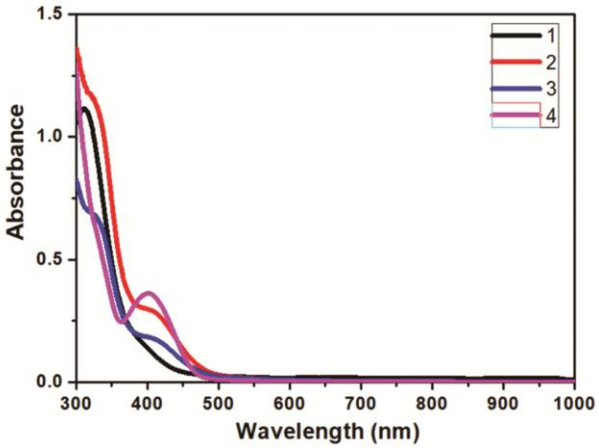

Fig. 1 — Electronic spectra of complexes **1-4** in (1.0×10^{-3} M) DMSO solution

Table 2 — Electrochemical data of complexes at RT in DMSO

Complex	E_{pc}(V)	E_{pa}(V)	$E_{(dpv)}$(V)
1	-0.975, -1.193	-0.676, -1.147	
2	-1.019	-0.677	+0.104, -0.801
3	-1.004	-0.658	+0.070, -0.817
4	-0.980	-0.695	+0.053, -0.779

Table 1 — FTIR spectral data of complexes 1-4

Complex	ν(OH)	ν(C=N)	ν(C=O)	ν(C-O)	ν(V=O)	ν(V-O)	ν(V-N)
1	3436	1604	1632	1289	952	432	417
2	3382	1596	1621	1301	975	484	445
3	3485	1606	1632	1300	972	459	409
4	3429	1605	1633	1298	973	444	410

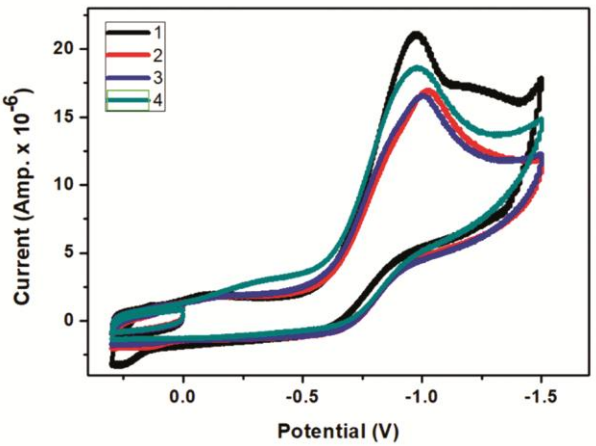

Fig. 2 — Cyclic voltammograms of complexes 1-4 in DMSO (1.0×10^{-3} M) at an Ag/AgCl electrode at a scan rate of 300 mVs^{-1} and temperature of 20 °C

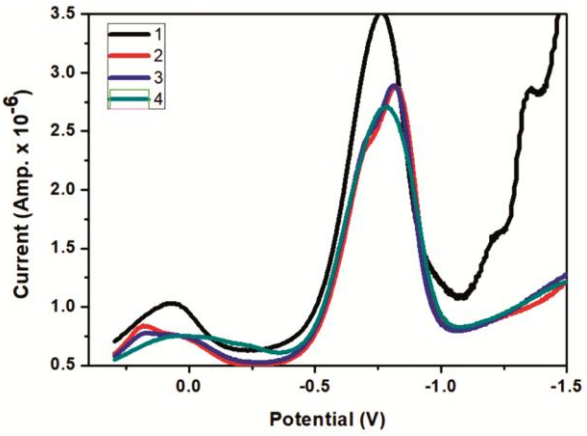

Fig. 3 — Differential pulse voltammograms of complexes **1-4** at 20 °C in DMSO (1.0×10^{-3} M) solution (pulse amplitude = 50 mV)

The reduction process exhibits one-electron transfer i.e., the reduction of vanadium(V) to vanadium(IV)[27]. In complexes **1** and **4** one cathodic peak is due to the reduction of ligand moiety. Such reduction processes were verified by DPV experiments and the curves are shown in Fig. 3. The reduction potential at - (0.753-0.8175 V) can be the one-electron reduction process from vanadium(V) to vanadium(IV). The CV of all complexes is without any response. Although, the less defined peak observed in DPV at positive potential is due to the reduction of ligand moiety.

Computational Study

Optimized structure of complexes

Geometry optimization complexes **1-4** have been performed using the density functional theory (DFT) method[28,29]. Optimized molecular structures are shown in Fig. 4 and the B3LYP calculated geometric parameters *viz.*, bond lengths, bond angles, optimized energies, frontier molecular orbitals (HOMO and LUMO) and energy gap (ΔE) have been also calculated using the B3LYP-6-31G/LanL2DZ levels using the Gaussian 09 program package. The vanadium(V) ion has a distorted octahedral coordination environment. The pro-ligand Schiff base acts as tridentate ligand (NOO) (L^{2-}) and maltol (L^{-}) acts as bidentate (OO) ligand. The donor atoms of pro-ligands (NOO) and hydroxyl oxygen atom of the complex whereas axial positions are occupied by a carbonyl oxygen atom of maltol and the oxygen atom of oxido group. In remaining complexes, axial positions are occupied by oxido O atom and O/N atom of tridentate Schiff base. The sum (Σ) of the transoid bond angles in all complexes are not equal to 360°, suggesting that the base plane is not perfectly square planar, in agreement with a distorted octahedral coordination geometry Table S1, Supplementary Data[30-32]. The transoid and cisoid angles are deviated from 180° and 90°, again confirming that the coordination geometry around vanadium(V) centre is distorted octahedral. Also, this six-coordinate oxidovanadium (V) complexes are tetragonally distorted ($T = R_{in}/R_{out}$).

HOMO-LUMO analysis

Interestingly, the singly occupied molecular orbital (SOMO/α-spin HOMO) is localized completely on the pro-ligand in **1** and **3** and on tilery on metal centre in **2** and **4** in maltol (co-ligand) containing complexes except in HOMO-3. HOMO-LUMO energies have been estimated to find out the energetic nature and energy distribution (Fig. S1, Supplementary Data). The HOMO frontier molecular HOMO represents electron releasing ability whereas LUMO gives information about the electron gain ability of the ligand. The estimated HOMO and LUMO energy values for complexes **1-4** are given in Table 3. The energy gap (ΔE) between HOMO and LUMO frontier orbitals is the critical parameter in evaluating the molecular electrical transport properties *viz.*, chemical reactivity, kinetic stability and softness-hardness of a chemical moiety. The chemical (global) hardness is a good indicator of chemical stability.

Global reactivity parameters

The estimated values of the reactivity descriptors of complexes **1-4** are given in Table 4. The energies of HOMO and LUMO frontier molecular orbitals are useful in quantum chemical calculations and are related to ionization potential (IP) and electron

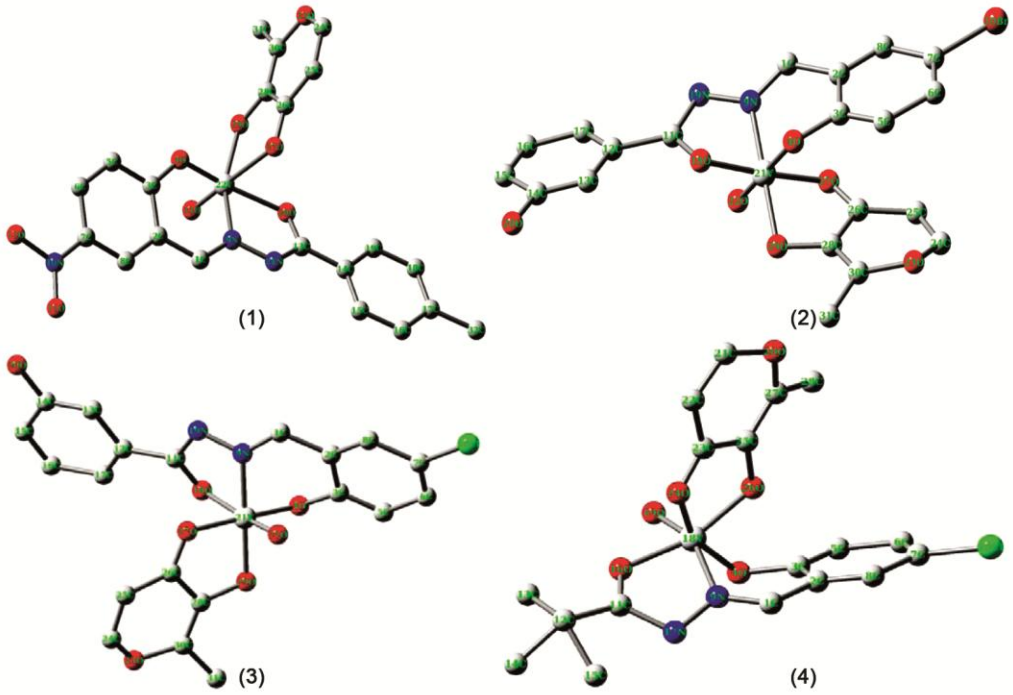

Fig. 4 — Optimized structures of complexes **1-4**

Table 3 — Natural electron configuration of complexes 1-4

Complex	Natural Electronic Configuration					Core	Valence	Rydberg
	4s	3d	4p	4d	5s			
1	0.22	3.59	0.37	0.09	-	17.974	4.183	0.093
2	0.24	3.86	0.42	0.12	-	17.977	4.521	0.125
3	0.23	3.59	0.37	0.09	-	17.977	4.194	0.099
4	0.24	3.80	0.39	0.10	0.01	17.975	4.434	0.107

Table 4 — Global reactivity descriptors vanadium complexes 1-4 in calculated by DFT/B3LYP/LANL2DZ basic

Molecular properties	Mathematical description	1	2	3	4
E_{HOMO} (eV)	Energy of HOMO	-3.362	-6.003	-3.844	-5.069
E_{LUMO} (eV)	Energy of LUMO	-3.360	-3.295	-2.956	-3.883
Energy gap (eV)	$\Delta E_g = E_{HOMO} - E_{LUMO}$	0.002	2.708	0.888	1.186
Ionization potential (eV)	$IP = -E_{HOMO}$	3.362	6.003	3.844	5.069
Electron Affinity (eV)	$EA = -E_{LUMO}$	3.360	3.295	2.956	3.883
Electronegativity (eV)	$(\chi) = -½ (E_{Homo} + E_{Lumo})$	3.361	4.649	3.400	4.476
Chemical Potentia (eV)	$\mu = ½ (E_{Homo} + E_{Lumo})$	-3.361	-4.649	-3.400	-4.476
Global Hardness (eV)	$(\eta) = - ½ (E_{Homo} - E_{Lumo})$	0.001	1.354	0.444	0.593
Softness (eV^{-1})	$(S) = 1/2\eta$	500	0.369	1.126	0.843
Electrophilicity index (ω)	$\omega = \mu^2/2\eta$	5648.16	7.98	13.01	16.89

affinity as $IP = -E_{HOMO}$ and $EA = -E_{LUMO}$. The other crucial chemical descriptors such as chemical potential (μ) the resistance to alternation in electron distribution are related to the stability and reactivity of a chemical moiety. The global softness (S) is the inverse of the hardness (η). The chemical species having a small ΔE is referred to as soft and with large ΔE as hard species. The electronegativity (χ) of a chemical molecule yields information about the negative of the partial derivative of the energy (E) of a molecule concerning the number of the electron (N) with a constant external potential (η). Similarly, the global electrophilicity (ω) descriptor gives the information about lowering of the energy due to maximal electron flow between donor and acceptor atoms[33]. These descriptors can be calculated from Koopman's theorem given in Table 3[34]. The negative chemical potential (μ) of the complexes (**1-4**)

suggests the stability of complexes. The magnitude of hardness reveals the resistance towards the distortion of the electron cloud of complexes with perturbation and less polarizability[35]. The values of ω are suggestive of good electrophile-nucleophile combination in complexes **1-4**.

Electron density

The surfaces of spin density all complexes (**1-4**) are shown Fig. 5. Most of the electron density is located on the vanadium(V) centre. The spin population, Mulliken population and natural population on the vanadium(V) centre are given in Table S2, Supplementary Data. Additionally, the natural bond order analysis of the complexes **1-4** was performed using B3LYP/LANL2DZ level basics set. The natural bond orbital (NBO) analysis is used to explore inter and intra molecular interactions among the bonds[36], which corresponds to a stabilizing donor-acceptor interaction[37]. The natural atomic charges of donor atoms are listed in Table S2. The maximum positive charge on V(V) centers in **1** found to be +0.696e. In all complexes, donor atoms have negative charges. According to NBO analysis, the natural electronic configuration of V is: [Core] 4s(0.22), 3d(3.59), 4p(0.37). Therefore, core electrons (18), valence electrons (4.183) on 4s, 3d and 4p orbitals and Rydberg electrons (0.093) mainly on 4p, 4d and 5p orbitals yield 22.89 electrons and +0.696 charge on V atom in **1**. The valence electrons and Rydberg electrons for other complexes (**1-4**) are listed in Table 4. This is persistent with the calculated natural charge on V atom 0.11 in complexes, which corresponds to the difference between 22.363 and the total no. of electrons in the isolated V atom 23e in **4**. On the perusal of data of Tables S2 and 3, it is found that the formal charges of the donor atoms indicate that the electron distribution is not confined to the coordination bonds as the values of DFT calculated formal charges of V centres are small-scale than +5. Scale decreases in the formal charge value are being the complexation, with charge transfer from vanadium to the ligand (MLCT).

Generally, V(V) centre in each complex plays as an electron acceptor in coordinating with pro-ligand (Schiff base) and maltol (as co-ligand). Electron density is transferred from the lone pair electron of donor atoms to the unoccupied orbitals on vanadium with lower stabilization energies.

Antidiabetic activity

α-Glucosidase inhibition activity

The α-glucosidase inhibition activity of complexes **1-4** was determined using the inhibition assay method[38,39]. The IC_{50} value for present complexes was evaluated from the percentage inhibition *vs.* concentration plot (Fig. 6) The IC_{50} values of complexes are shown in Table 5. In the same Table, α-glucosidase activity is also listed. The observed trend in α-glucosidase activity is: **1** > **3** > **4** > **2**. Complex **1** showed the highest α-glucosidase activity and **2** showed the lowest activity. The observed trend inactivity is similar to the energy gap trend of these

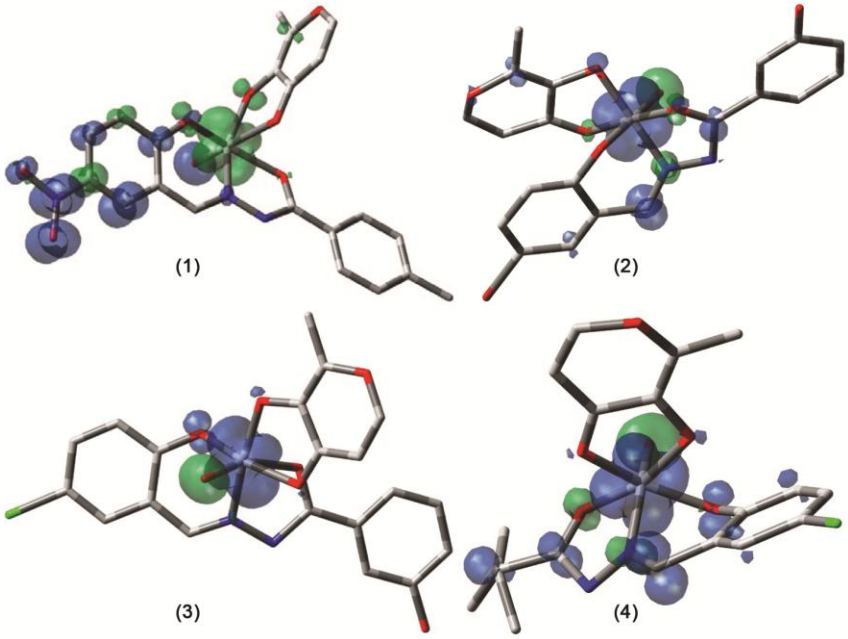

Fig. 5 — Spin density of complexes **1-4**

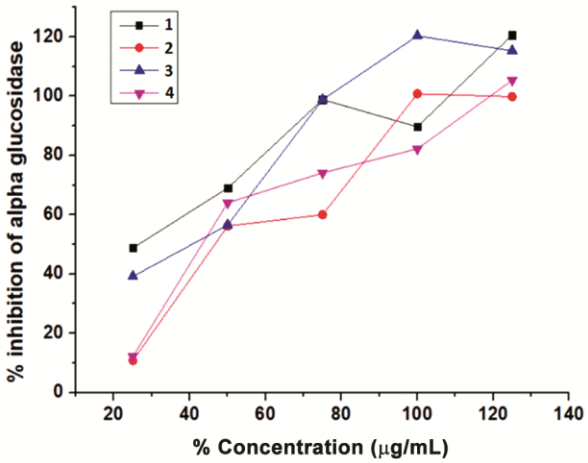

Fig. 6 — α-Glucosidase inhibitory activity of complexes **1-4**

Table 5 — Antidiabetic parameters of complexes 1-4

Complex	IC_{50} (µg/mL)	α-glucosidase activity ($µg^{-1}$)
1	25.78	38.79
2	46.86	21.34
3	40.18	24.89
4	43.63	22.92

complexes. For complex **1** the energy gap is (ΔE) minimum and for **2** is maximum. The ΔE is also associated with the global softness (S). The value of S is highest for **1** and lowest for **2**. Therefore, these observations of crucial electronic parameters supported the trend of α-glucosidase reactivity. These complexes bind the α-glucosidase enzymes in the active or allosteric site through the vacant coordination site of vanadium(V) center in complexes. After binding, the establishment of H-bonding and hydrophobic interactions establish the inhibitor cooperatively[39]. Then mode of inhibition was checked for complex with the best IC_{50}. The α-glucosidase activity values are comparable with those reported in the literature[38-41].

α-Amylase inhibition activity

The percentage of α-amylase enzyme activity of complexes **1-4** was screened by the reported inhibition assay method[40,41]. The percentage inhibition *vs.* concentration is shown in Fig. 7. From this plot, IC_{50} value was determined and presented in Table 6. In the same table value of α-amylase inhibition activity parameters is also listed in Table 6. The found trend in α-amylase of present complexes is similar to that of α-glucosidase inhibition activity. This trend is parallel to the trend of global reactivity parameters. Complex **1** is the global highest soft less hard molecule that showed the α-amylase activity. All

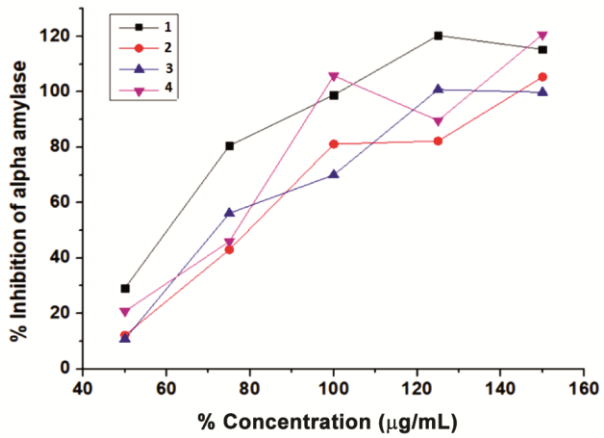

Fig. 7 — α-Amylase inhibitory activity of complexes **1-4**

Table 6 — Antidiabetic parameters of complexes 1-4

Complex	IC_{50} (µg/mL)	α-amylase activity ($µg^{-1}$)
1	60.01	16.66
2	80.40	12.44
3	71.97	13.89
4	76.66	13.04

complexes showed good α-amylase activity. The square pyramidal geometry of present complexes may bind near the active sites through hydrogen bonds or other hydrophobic interactions. Consequently, block the access to the active site of the enzyme is no longer active for hydrolysis of the starch molecule. The α-amylase activities of present complexes are in good agreement with those reported in the literature[38-41].

Conclusions

We have synthesized **1-4** oxidovanadium(V) complexes with different ligands using *in-situ* process. The recent interest of inorganic, bioinorganic chemists and pharmacologists in antidiabetic oxidovanadium(V) complexes has resulted in synthesis, characterization, and exploration of antidiabetic proportions of four new oxidovanadium(V) complexes. All the complexes have been characterized by various physicochemical techniques. The molecular structures show the presence of six donor atoms around the oxidovanadium(V) and hence octahedral geometry is proposed. In complexes, **1-4** d-d absorption bands were not observed in all complexes being d^0 vanadium systems. The V ions in complexes **1-4** are in octahedral coordination. In complexes, the **1-4** reduction process exhibits one-electron transfer i.e. the reduction of vanadium(V) to vanadium(IV). The complexes show moderate *in vitro* α-glucosidase and α-amylase inhibition. Complex **3** has an interesting

insulin-like activity. Hence, we may conclude that these complexes may be considered antidiabetic agents.

Supplementary Data

Supplementary data associated with this article are available in the electronic form at http://nopr.niscair.res.in/jinfo/ijca/IJCA_61(03)YYYY-YYYY_SupplData.pdf.

Acknowledgment

The authors are thankful to CDRI Lucknow for microanalysis and IIT Ropar for ESI mass analysis.

References

1 Kim A T & Kim D O, *Int J Biol Macromol*, 133 (2019) 732.
2 Kumar S, Syed A, Andotra S, Kaur R, Vikas & Pandey S K, *J Mol Struct*, 1154 (2018) 165.
3 Pessoaa J C, Etcheverry S & Gambino D, *Coord Chem Rev*, 301 (2015) 24.
4 Mjos K D & Orvig C, *Chem Rev*, 114 (2014) 4540.
5 Nielsen F H, *In Metal Ions in Biological Systems: Vanadium and Its Role in Life*, Vol 31, Sigel H & Sigel A (Eds.), (Marcel Dekker, New York) 1995, p 543.
6 Orvig C, Thompson K H, Battell M & McNeill J H, *Metal Ions in Biological Systems: Vanadium and Its Role in Life*, Vol 31, Sigel H & Sigel A (Eds.), (Marcel Dekker, New York) 1995, p 575.
7 Hussen A, *J Coord Chem*, 59 (2006) 157.
8 Karthikeyan S, Prasad M J, Poojary D & Bhat B S, *Bioorg Med Chem*, 14 (2006) 7482.
9 Singh K, Barwa M S & Tyagi P, *Eur J Med Chem*, 41 (2006) 1.
10 Pannerselvam P, Nair R R, Vijayalakshmi G, Subramanian E H & Sridhar S K, *Eur J Med Chem*, 40 (2005) 225.
11 Sridhar S K, Saravan M & Ramesh A, *Eur J Med Chem*, 36 (2001) 615.
12 Pandeya S N, Sriram D, Nath G & Declercq E, *Eur J Pharmacol*, 9 (1999) 25.
13 Mladenova R, Ignatova M, Manolova N, Petrova T & Rashkov I, *Eur Polym J*, 38 (2002) 989.
14 Walsh O M, Meegan M J, Prendergast R M & Nakib T A, *Eur J Med Chem*, 31 (1996) 989.
15 Cacic M, Molnar M, Sarkanj B, Has-Schon E & Rajkovic V, *Molecules*, 15 (2010) 6795.
16 Dave S & Bansal N, *Int J Curr Pharm Res*, 5 (2013) 6.
17 Apostolidis E, Kwon Y I I & Shetty K, *Asia Pac J Clin Nutr*, 15 (2006) 433.
18 Tripathi I P, Mishra M K, Tripathi R, Mishra C, Kamal A, Shastri L, Dwivedi A, Shukla U K & Pandeya K B, *Res J Chem Sci*, 4 (2014) 13.
19 Geary W J, *Coord Chem Rev*, 3 (1971) 81.
20 Seena E B, Mathew N, Kuriakose M & Kurup M R P, *Polyhedron*, 27 (2008) 1455.
21 Sasmal P K, Patra A K, Nethaji M & Chakravarty A R, *Inorg Chem*, 46 (2007) 11112.
22 Bhattacharya S & Ghosh T, *Indian J Chem*, 38A (1999) 601.
23 Trian G D, EI. Tolis E I & Terzis A, *Inorg Chim Acta*, 43 (2004) 79.
24 Jadeja R N & Shah J R, *Polyhedron*, 26 (2004) 1677.
25 Dinda H, Sengupta P, Ghosh S & Mak T C W, *Inorg Chem*, 41 (2002) 1684.
26 Samanta S, Ghosh D, Mukhopadhyay S, Endo A, Weakley T J R & Chaudhury M, *Inorg Chem*, 42 (2003) 1508.
27 Riechel T L, Hayes L J D & Sawyer D T, *Inorg Chem*, 15 (1976) 1900.
28 Hay P J & Wadt W R, *J Chem Phys*, 82 (1985) 270.
29 Frisch M J, Trucks G W, Schlegel H B, Scuseria G E, Robb M A, Cheeseman J R, Scalmani G, Barone V, Mennucci B, Petersson G A, Nakatsuji H, Caricato M, Li X, Hratchian H P, Izmaylov A F, Bloino J, Zheng G, Sonnenberg J L, Hada M, Ehara M, Toyota K, Fukuda R, Hasegawa J, Ishida M, Nakajima T, Honda Y, Kitao O, Nakai H, Vreven T, Montgomery Jr J A, Peralta J E, Ogliaro F, Bearpark M, Heyd J J, Brothers E, Kudin K N, Staroverov V N, Kobayashi R, Normand J, Raghavachari K, Rendell A, Burant J C, Iyengar S S, Tomasi J, Cossi M, Rega N, Millam J M, Klene M, Knox J E, Cross J B, Bakken V, Adamo C, Jaramillo J, Gomperts R, Stratmann R E, Yazyev O, Austin A J, Cammi R, Pomelli C, Ochterski J W, Martin R L, Morokuma K, Zakrzewski V G, Voth G A, Salvador P, Dannenberg J J, Dapprich S, Daniels A D, Farkas O, Foresman J B, Ortiz J V, Cioslowski J & Fox D J, Gaussian 09, Revision D.01, Gaussian Inc., Wallingford CT, (2009).
30 Ramakrishnan S & Palaniandavar M, *Dalton Trans*, 29 (2008) 3866.
31 Murphy B, Aljabri M, Ahmed A M, Murphy G, Hathaway B J, Light M E, Geilbrich T, Hursthouse M B, *Dalton Trans*, 2 (2006) 357.
32 Ramakrishnan S, Shakthipriya D, Suresh E, Periasamy V S, Akbarsha M A & Palaniandavar M, *Inorg Chem*, 50 (2011) 6458.
33 Hathaway B J & Hodgson P G, *Polyhedron*, 35 (1973) 4071.
34 Par R G & R.G. Pearson R G, *J Am Chem Soc*, 105 (1983) 7512.
35 Koopmans T A & Oie Z U, *Physica*, 1 (1934) 104.
36 Pearson R G, *Chem Sci*, 117 (2005) 369.
37 Weinhold F & Landis C, *Valency and bonding: A Natural Bond Orbital Donor-Acceptor Perspective*, (Cambridge University Press Cambridge) 2005.
38 Tripathi I P, Kamal A, Mishra M K, Dwivedi A, Tripathi R, Mishra C & Shastri L, *Ind J Appl Res*, 4 (2014) 66.
39 Patel N, Prajapati A K, Jadeja R N, Patel R N, Patel S K, Tripathi I P, Dwivedi N, Gupta V K & Butcher R J, *Polyhedron*, 180 (2020)114434.
40 Patel N, Prajapati A K, Jadeja R N, Patel R N, Patel S K, Gupta V K, Tripathi I P & Dwivedi N, *Inorg Chim Acta*, 493 (2019) 20.
41 Patel N, Prajapati A K, Jadeja R N, Tripathi I P & Dwivedi N, *J Coord Chem*, 73 (2020) 1131.